

Establishment of a steroid binding assay for membrane progesterone receptor alpha (PAQR7) by using graphene quantum dots (GQDs)

メタデータ	言語: eng 出版者: 公開日: 2022-06-14 キーワード (Ja): キーワード (En): 作成者: Jyoti, Md. Maisum Sarwar, Rana, Md. Rubel, Ali, Md. Hasan, Tokumoto, Toshinobu メールアドレス: 所属:
URL	http://hdl.handle.net/10297/00029002

1
2
3
4
5
6
7
8
9
10
11
12
13
14
15
16
17
18
19

Establishment of a steroid binding assay for membrane progesterone receptor alpha (PAQR7) by using graphene quantum dots (GQDs)

Md. Maisum Sarwar Jyoti, Md. Rubel Rana, Md. Hasan Ali and Toshinobu Tokumoto*

Integrated Bioscience Section, Graduate School of Science and Technology, National University Corporation, Shizuoka University, 836 Ohya, Suruga-ku, Shizuoka, 422-8529 Japan

*Corresponding author. Tel: +81-54-238-4778; Fax: +81-54-238-4778.

E-mail addresses: tokumoto.toshinobu@shizuoka.ac.jp (T. Tokumoto).

20

21 **ABSTRACT**

22 Currently, semiconductor nanoparticles known as quantum dots (QDs) have attracted interest
23 in various application fields such as those requiring sensing properties, binding assays, and
24 cellular imaging and are the very important in the acceleration of drug discovery due to their
25 unique photophysical properties. Here, we applied graphene quantum dots (GQDs) for the
26 binding assay of membrane progesterone receptor alpha (mPR α), one of the probable
27 membrane receptors that have potential in drug discovery applications. By coupling the
28 amino groups of mPR α with GQDs, we prepared fluorogenic GQD-conjugated mPR α (GQD-
29 mPR α). When mixed with a progesterone-BSA-fluorescein isothiocyanate conjugate (P4-
30 BSA-FITC) to check the ligand receptor binding activity of GQD-mPR α , fluorescence at 520
31 nm appeared. The fluorescence at 520 nm was reduced by the addition of free progesterone
32 into the reaction mixture. GQD-coupled BSA (GQD-BSA) did not show a reduction in
33 fluorescence at 520 nm. The results demonstrated the formation of a complex of GQD-mPR α
34 and P4-BSA-FITC with ligand receptor binding. We established a ligand binding assay for
35 membrane steroid receptors that is applicable for high-throughput assays.

36

37 *Keywords:* graphene quantum dots, membrane progesterone receptor, progesterone, FRET,
38 steroids

39

40

41 **1. Introduction**

42 A group of steroid hormones, progestins, have a variety of functions in the regulation of the
43 reproductive function of the body [1,2]. The natural progestin progesterone plays an
44 important role in regulating egg maturation and the menstrual cycle along with the sex steroid
45 estrogen in humans [3]. Synthetic progestin imitates the effect of progesterone and controls
46 reproductive tissues in female and male vertebrates. Thus, progestins have been applied as
47 fertility control treatments, contraceptives, and anticancer drugs [4]. More recently,
48 progestins have attracted attention for Alzheimer's hormone therapy [5]. Currently, it is
49 becoming clear that progestins have some nongenomic effects mediated by membrane
50 progestin receptors (mPRs) on plasma and induce rapid intracellular changes [6,7].

51 mPRs are members of a group of cell surface receptors, i.e., the progestin and the
52 AdipoQ receptor (PAQR) family [8]. The receptor containing the seventh gene of the PAQR
53 family, mPR α (PAQR7), is one of the protein subtypes that have been suggested to be
54 involved in physiological roles in reproductive tissues [6]. Although the 3D structure of
55 PAQR7 has still not been determined, computer modeling predicts that the proteins have
56 seven typical transmembrane domains as G protein coupled receptors (GPCRs) [9,10].

57 Many mPR-mediated nongenomic actions of progestins have been demonstrated, such
58 as induction of oocyte maturation [11,12], quick activation signaling of breast cancer cells
59 [7], mammalian sperm hypermotility [13], and induction of lordosis (female mating
60 acceptance behavior) [14]. The action of neurosteroids in the brain is of particular interest. A
61 progestin in the brain, allopregnanolone, is attracting attention as a therapeutic drug for
62 Alzheimer's disease [5]. Recently, it was suggested that the antiapoptotic actions of
63 allopregnanolone on neuronal cells are mediated through mPRs [15]. Additionally, it was

64 demonstrated that allopregnanolone promotes the development of chick Purkinje cells via
65 mPR [16].

66 The mPR molecule is also drawing attention in relation to cancer. Cancer-related
67 reports include high expression levels of mPR molecules in breast cancer, ovarian cancer and
68 brain cancer [7]. Thus, it is suggested that the mPR molecule should be used as a marker for
69 cancer diagnosis [17]. A notable report on the action of progesterone on cancer cells showed
70 that progesterone suppresses cancer infiltration, and it has been shown that this effect is
71 transmitted via mPR [18].

72 Quantum dots (QDs) are very small semiconductor particles a few nanometers in size
73 that have optical and electronic properties that differ from those of larger particles due to
74 quantum mechanics [19]. When QDs are illuminated by UV light, an electron in the quantum
75 dot can be excited to a state of higher energy and release its energy by the emission of light.
76 The color of the light depends on the energy difference between the conductance band and
77 the valence band of QDs.

78 One application of quantum dots in biology is as donor fluorophores in Förster
79 resonance energy transfer (FRET), where the large extinction coefficient and spectral purity
80 of these fluorophores make them superior to molecular fluorophores [20]. It is also worth
81 noting that the broad absorbance of QDs allows for the selective excitation of the QD donor
82 and minimum excitation of a dye acceptor in FRET-based studies [21]. The applicability of
83 the FRET model, which assumes that the quantum dot can be approximated as a point dipole,
84 has recently been demonstrated [22].

85 As a class of zero-dimensional nanomaterials, graphene quantum dots (GQDs) have
86 been discovered recently. GQDs along with their doped or functionalized nanocomposites
87 have emerged as the most promising nanomaterials in several fields because of their

88 extraordinary optical, thermal, and electronic properties, such as electronics [23,24], energy
89 storage [25], catalysis [26], materials science [27] and biomedical engineering [28]. More
90 recently, fluorescence assays using fluorophores or transition metal chalcogenide-based QDs
91 have become significant for achieving high sensitivity and rapid response to metal ion and
92 organic detection [29,30].

93 Previously, we succeeded in the production and purification of recombinant human
94 mPR α with progesterone binding activity by using a yeast protein expression system [31].
95 Since the binding assay system for mPR α is expected to be applied for screening new
96 compounds for pharmaceuticals, we attempted to establish a new assay system using
97 recombinant human mPR α protein and QDs in this study. Here, we produced soluble QD-
98 mPR α and established a new steroid binding assay with fluorescently labeled progesterone.

99

100 **2. Materials and methods**

101 *Materials*

102 Citric acid, N-(3-Dimethylaminopropyl)-N'-ethylcarbodiimide hydrochloride, N-
103 hydroxysuccinimide and steroids (corticosterone, cortisol, progesterone, testosterone, 17 β -
104 estradiol, 17 α -methyl-testosterone, mifepristone) were purchased from Sigma Aldrich
105 Chemicals (St. Louis, MO). 17 α -hydroxyprogesterone and other chemicals were purchased
106 from Wako Pure Chemical Industries, Ltd. (Osaka, Japan). Spectra 3.5 kDa dialysis
107 membranes were purchased from Spectra Laboratories Inc. (USA).

108

109 *Preparation of hmPR α*

110 Human mPR α (hmPR α) proteins were expressed and purified as previously described
111 [31].

112

113 *Preparation of GQDs*

114 The GQDs were prepared by using direct pyrolyzation of citric acid [32]. In a typical
115 procedure of GQD preparation, 2 g of citric acid was added into a 100 mL round-bottom
116 flask and heated to 200 °C by using a drying oven. The solid crystal citric acid became liquid
117 and turned yellowish after 5 min. Then, an orange color appeared after heating for 20 min,
118 indicating the formation of GQDs. In addition, different reaction times ranging from 20 to 45
119 min were examined, and a reaction time of 25 min was chosen in this study to fabricate the
120 as-prepared GQDs with a high quantum yield (QY). Excess heating was strictly avoided
121 because overheating may possibly cause the formation of graphene oxides. The obtained
122 orange liquid containing GQDs was then added dropwise into 100 mL of 10 g/L sodium
123 hydroxide (NaOH) solution under vigorous stirring. After neutralization to pH 7.0 with
124 NaOH, an aqueous solution of GQDs was obtained and preserved in the dark at 4 °C for
125 further use. The QY of prepared GQDs was determined by using fluorescein as the standard
126 solution ($\Phi=0.79$). The QY was calculated to be 0.124, which was same as the original report
127 [32].

128

129 *Preparation of GQDs coupled mPR α*

130 The GQD-labeled mPR α (GQD-mPR α) was prepared by coupling the amine group/N-
131 terminus of mPR with the carboxylic acid group of GQDs using the standard N-ethyl-N'-(3-
132 (dimethylamino) propyl) carbodiimide (EDC)/N-hydroxysuccinimide (NHS) reaction at room

133 temperature at pH 6.0 (Fig. 1A) [33]. As a control, GQD-labeled BSA (GQD-BSA) was
134 prepared in the same manner as GQD-mPR α . Briefly, EDC and NHS were added to the GQD
135 solution under vigorous stirring (on a small scale: 3 mg of EDC and 4 mg of NHS for 10 mL
136 of GQD solution, on a large scale: 20 mg of EDC and 25 mg of NHS for 60 mL of GQD
137 solution). Then, mPR α or BSA solution (on a small scale: 100 μ L of 0.43 mg/mL mPR α
138 solution or 0.5 mg/mL BSA solution, on a large scale: 60 mL of 0.14 mg/mL mPR α solution)
139 was added to the GQD solution, and the reaction was performed for 2 h under vigorous
140 stirring at room temperature. Then, the final solution was dialyzed in a 3.5 kDa dialysis bag
141 for 24 h (dialysate was replaced with DDW every 8 h) to remove the unreacted chemicals.
142 Prepared GQD-mPR α and GQD-BSA were stored at -30 $^{\circ}$ C.

143

144 *Preparation of FITC-labeled progesterone-coupled BSA (P4-BSA-FITC)*

145 P4-BSA-FITC was prepared by a standard reaction for FITC labeling of progesterone-
146 coupled BSA (4-Pregnen-3,20-Dione 3-O-Carboxymethyloxime/BSA, Steraloids Inc. USA).

147

148 *Binding assay using mPR α -GQDs and P4-BSA-FITC*

149 Except for the test chemicals, mPR α -GQDs and P4-BSA-FITC were mixed in a
150 reaction mixture of phosphate buffer, pH 7.4. To a well of a 96-well plate, 2 μ l of test
151 compound dissolved in ethanol was applied. Then, 98 μ l of reaction mixture (final
152 concentrations of mPR α -GQDs at 9 μ g/ml mPR α , P4-BSA-FITC at 14 μ g/ml BSA) was
153 added and mixed (Fig. 1B). The prepared reaction mixture was incubated in the dark for 2 hrs
154 at room temperature. Then, the fluorescence intensity of each well was measured by a

155 fluorescence microplate reader (Varioskan™ LUX, Thermo Scientific, Waltham, USA) at an
156 excitation wavelength of 370 nm and an emission wavelength of 520 nm.

157

158 **3. Results**

159 *3.1 Functionalization of GQDs with mPR α*

160 GQDs were manually prepared from citric acids. The preparation of GQDs was
161 confirmed by visible fluorescence under UV light and by fluorescence scanning. GQDs
162 solution showed blue color when excited by violet light bulb (Fig. 1A). The fluorescent peak
163 was observed at 460 nm by excitation at 360 nm (Fig. 1B). Recombinant hmPR α was
164 purified by two steps of column chromatography, Ni-NTA column and Cellufine Amino
165 column chromatography, which was previously determined to be an effective resin for the
166 purification of mPR α protein (Fig. 1C) [34]. Then, we tried to couple prepared GQDs with
167 purified mPR α proteins. By a standard EDC/NHS reaction, GQDs were coupled with mPR α
168 proteins on their amino groups through peptide bonds (Fig. 1C). Formation of peptide bonds
169 between GQDs and mPR α proteins was confirmed by FTIR analysis (Fig. 1D). The peaks
170 shown in Figure 1D at 1400 and 1593cm⁻¹ indicate the presence of C=C stretching and
171 carboxyl (C=O) group, respectively. A broad peak at 3400cm⁻¹ confirms the characteristic of
172 hydroxy (-OH) group from carboxyl group. After surface functionalization of mPR α , a strong
173 attached peak at 1644cm⁻¹ that assigned as the amide group appeared with the increased
174 intensity at 1593cm⁻¹. In addition, GQD-mPR α showed another peak at 1710cm⁻¹ which
175 correspond to the C-N stretching. These specific peaks strongly suggested that prepared
176 GQDs successfully coupled with mPR α . By TEM observation, average size of GQD-mPR α
177 particle was determined as 9.5 nm (Fig. 1E).

178 Then, we analyzed the spectrometric characteristics of GQD-mPR α prepared in this
179 study. The maximum fluorescence intensity of the prepared GQD-mPR α was observed at an
180 excitation wavelength of 370 nm, and the peak fluorescence from GQD-mPR α was observed
181 at 470 nm (Fig. 2A). The excitation wavelength was slightly shifted to a longer wavelength of
182 360 nm for free GQDs.

183 *3.2 Specific binding of progesterone in P4-BSA-FITC with GQD-mPR α .*

184 Then, we tried to detect the binding of GQD-mPR α and P4-BSA-FITC. We set the
185 excitation wavelength for the reaction mixture to 370 nm, which was the maximum excitation
186 wavelength of GQD-mPR α . Scanning of the GQD-mPR α and P4-BSA-FITC reaction
187 mixture showed twin peaks when excited at 370 nm (Fig. 2B). The first peak at 470 nm
188 corresponded to free GQD-mPR α . The second peak at 520 nm corresponded to the mixed
189 fluorescent peak of GQD and FITC. The second peak of fluorescence at 520 nm was reduced
190 by the addition of free progesterone (Fig. 2B). The results suggested that a part of this peak
191 was from FITC-labeled progesterone that bound with GQD-mPR α by exciting FITC by
192 fluorescence from GQDs with a FRET mechanism. It is highly possible that the reduction in
193 fluorescence was caused by competitive binding of free progesterone to the steroid binding
194 site of mPR α and release of P4-BSA-FITC (Fig. 3). According the results, we measured the
195 excitation wavelength as 370 nm and the emission wavelength as 520 nm for the binding
196 assay. Under this condition, GQD-mPR α showed a reduction in fluorescence intensity at 520
197 nm upon the addition of the mPR α agonist progesterone. In contrast, GQD-BSA showed no
198 change in fluorescence intensity at 520 nm (Fig. 2C and 2D). The specificity of this assay
199 was further confirmed by assays of various steroids and compounds related to progesterone
200 (Fig. 2E). Only progesterone and 17 α -hydroxyprogesterone showed competitive binding
201 activity against P4-BSA-FITC. In contrast, other steroids, estradiol, testosterone,

202 corticosterone and cortisol, showed no activity even at high concentrations. Thus, we
203 concluded that we succeeded in detecting the binding of mPR α and its agonist progesterone.
204 A model for the mechanism of changing fluorescent intensity by changing of specific binding
205 of P4 in P4-BSA-FITC and steroid binding site in GQD-mPR α (Fig. 3). The decrease of
206 fluorescent that caused by FRET between GQD and FITC induced by binding of free P4.

207

208 **4. Discussion**

209 Previously, we succeeded in purifying a relatively large amount of human mPR α
210 protein with hormonal binding activity [31]. By using purified recombinant proteins, we
211 established a way to detect the specific binding of steroids to the mPR α protein, which is
212 expected to enable high-throughput screening of mPR α agonists or antagonists. The
213 selectivity of steroids specific for progestins was confirmed. Among the four kinds of
214 steroids, only progesterone and its analogs showed binding. In contrast, estradiol-17 β ,
215 testosterone and cortisol did not show any binding activity, as reported by the results of a
216 binding assay using ³H-labeled steroid and recombinant proteins expressed in cancer cells
217 [6]. Antagonists against nuclear progesterone receptor (PR), mifepristone (RU486), did not
218 show competitive binding activity against P4-BSA-FITC. This result was consistent with
219 reported results that showed that mifepristone did not bind to mPR α [6]. These results
220 suggested that our established binding assay can detect the specific binding of progesterone
221 to its steroid binding site.

222 We have already established and reported several assays for agonists or antagonists of
223 mPR α [35]. Initially, we reported a steroid binding assay using ³H-labeled steroids and cell
224 membranes containing recombinant mPR α [36]. Although the assay gave us confident

225 results, manual operation using cell culture and test tubes is laborious and assaying large
226 numbers of samples is difficult. Classical techniques and *in vitro* oocyte maturation assays
227 using oocytes are still useful for analyzing mPR-interacting chemicals [37,38]. However, this
228 technique requires fully developed oocytes that are ready to mature, which means that female
229 animals must be ready to spawn. Thus, the method requires a large number of animals kept
230 under appropriate conditions, and it is almost impossible to perform a large number of assays.
231 We also found *in vivo* induction of oocyte maturation and ovulation by simply adding
232 chemicals into the water in zebrafish [39]. Although this method enables the assay of the
233 effect of chemicals on mPRs *in vivo*, the number of fish required for the assay is extremely
234 high. Thus, the application of *in vivo* assays is limited for several selected compounds. Most
235 recently, we established a cell-based chemiluminescent assay using a functionally modified
236 luciferase gene [40]. The assay enables the detection of the function of agonists that induce
237 changes in intracellular cAMP levels. However, the assay demands high costs, and it is
238 difficult to obtain stable data due to difficulties in preparing cells under constant conditions.
239 The established assay in this study using purified recombinant protein enables large numbers
240 of assays with the same batch of purified fractions. Even though it can be improved on a
241 smaller scale, more than 10 96-well plate assays are enabled by using the same preparation of
242 GQD-mPR α . Thus, a highly reproducible assay for 1000 tests is enabled even on a laboratory
243 scale. The changes in fluorescent intensity was small for this assay. However, high
244 reproductivity recovered this disadvantage and produced significant differences. It can be
245 speculated that a small magnitude of change reflects the exchange of progesterone on a single
246 steroid binding site on mPR α .

247 In this study, we established a binding assay for human mPR α that enables the high-
248 throughput screening of compounds that act on mPR α . This assay will lead to the
249 identification of new compounds for pharmaceuticals.

250

251 **Declaration of competing interest**

252 The authors declare that there are no conflicts of interest.

253

254 **Acknowledgments**

255 This work was supported by Grants-in-Aid for Scientific Research on Priority Areas
256 from the Ministry of Education, Culture, Sports, Science and Technology of Japan; JSPS
257 KAKENHI Grant Number 20K06719 (to TT).

258 We would like to thank Dr. Ankan Dutta Chowdhury for valuable suggestions for
259 GQD preparation and conducting FTIR analysis and TEM observation. We also thank Prof.
260 Enock Y. Park for suggestions and encouragement during the study.

261

262 **References**

- 263 [1] O.M. Conneely, B. Mulac-Jericevic, J.P. Lydon, Progesterone-dependent regulation of
264 female reproductive activity by two distinct progesterone receptor isoforms, *Steroids* 68
265 (2003) 771-778.
- 266 [2] B. Gellersen, M.S. Fernandes, J.J. Brosens, Non-genomic progesterone actions in female
267 reproduction, *Human Reproduction Update* 15 (2009) 119-138.
- 268 [3] F.Z. Stanczyk, All progestins are not created equal, *Steroids* 68 (2003) 879-890.
- 269 [4] H. Kuhl, Pharmacology of estrogens and progestogens: influence of different routes of
270 administration, *Climacteric* 8 (2005) 3-63.
- 271 [5] T. Wang, J. Yao, S.H. Chen, Z.S. Mao, R.D. Brinton, Allopregnanolone Reverses
272 Bioenergetic Deficits in Female Triple Transgenic Alzheimer's Mouse Model,
273 *Neurotherapeutics* 17 (2020) 178-188.
- 274 [6] P. Thomas, Y. Pang, J. Dong, P. Groenen, J. Kelder, J. de Vlieg, Y. Zhu, C. Tubbs,
275 Steroid and G protein binding characteristics of the seatrout and human progestin
276 membrane receptor alpha subtypes and their evolutionary origins, *Endocrinology* 148
277 (2007) 705-718.
- 278 [7] P. Valadez-Cosmes, E.R. Vazquez-Martinez, M. Cerbon, I. Camacho-Arroyo, Membrane
279 progesterone receptors in reproduction and cancer, *Molecular and Cellular*
280 *Endocrinology* 434 (2016) 166-175.
- 281 [8] Y.T. Tang, T. Hu, M. Arterburn, B. Boyle, J.M. Bright, P.C. Emtage, W.D. Funk, PAQR
282 proteins: a novel membrane receptor family defined by an ancient 7-transmembrane pass
283 motif, *J Mol Evol* 61 (2005) 372-380.
- 284 [9] J. Bockaert, J.P. Pin, Molecular tinkering of G protein-coupled receptors: an evolutionary
285 success, *Embo Journal* 18 (1999) 1723-1729.
- 286 [10] Y. Zhu, C.D. Rice, Y. Pang, M. Pace, P. Thomas, Cloning, expression, and
287 characterization of a membrane progestin receptor and evidence it is an intermediary in
288 meiotic maturation of fish oocytes, *Proc Natl Acad Sci U S A* 100 (2003) 2231-2236.

- 289 [11] M. Tokumoto, Y. Nagahama, P. Thomas, T. Tokumoto, Cloning and identification of a
290 membrane progesterin receptor in goldfish ovaries and evidence it is an intermediary in
291 oocyte meiotic maturation, *General and Comparative Endocrinology* 145 (2006) 101-108.
- 292 [12] Y. Zhu, J. Bond, P. Thomas, Identification, classification, and partial characterization of
293 genes in humans and other vertebrates homologous to a fish membrane progesterin
294 receptor, *Proc Natl Acad Sci U S A* 100 (2003) 2237-2242.
- 295 [13] C. Tubbs, P. Thomas, Progesterin Signaling through an Olfactory G Protein and
296 Membrane Progesterin Receptor-alpha in Atlantic Croaker Sperm: Potential Role in
297 Induction of Sperm Hypermotility, *Endocrinology* 150 (2009) 473-484.
- 298 [14] C.A. Frye, A.A. Walf, A.S. Kohtz, Y. Zhu, Progesterone-facilitated lordosis of estradiol-
299 primed mice is attenuated by knocking down expression of membrane progesterin
300 receptors in the midbrain, *Steroids* 81 (2014) 17-25.
- 301 [15] P. Thomas, Y.F. Pang, Anti-apoptotic Actions of Allopregnanolone and Ganaxolone
302 Mediated Through Membrane Progesterone Receptors (PAQRs) in Neuronal Cells,
303 *Frontiers in Endocrinology* 11 (2020).
- 304 [16] S. Haraguchi, M. Kamata, T. Tokita, K.I. Tashiro, M. Sato, M. Nozaki, M. Okamoto-
305 Katsuyama, I. Shimizu, G. Han, V.S. Chowdhury, X.F. Lei, T. Miyazaki, J.R. Kim-
306 Kaneyama, T. Nakamachi, K. Matsuda, H. Ohtaki, T. Tokumoto, T. Tachibana, A.
307 Miyazaki, K. Tsutsui, Light-at-night exposure affects brain development through pineal
308 allopregnanolone-dependent mechanisms, *Elife* 8 (2019).
- 309 [17] M.X. Xie, X.Z. Zhu, Z.F. Liu, M. Shrubsole, V. Varma, I.A. Mayer, Q. Dai, Q. Chen,
310 S.J. You, Membrane Progesterone Receptor Alpha as a Potential Prognostic Biomarker
311 for Breast Cancer Survival: A Retrospective Study, *Plos One* 7 (2012).
- 312 [18] L. Zuo, W. Li, S. You, Progesterone reverses the mesenchymal phenotypes of basal
313 phenotype breast cancer cells via a membrane progesterone receptor mediated pathway,
314 *Breast Cancer Res* 12 (2010) R34.
- 315 [19] E. Petryayeva, W.R. Algar, I.L. Medintz, Quantum Dots in Bioanalysis: A Review of
316 Applications Across Various Platforms for Fluorescence Spectroscopy and Imaging,
317 *Applied Spectroscopy* 67 (2013) 215-252.
- 318 [20] U. Resch-Genger, M. Grabolle, S. Cavaliere-Jaricot, R. Nitschke, T. Nann, Quantum
319 dots versus organic dyes as fluorescent labels, *Nature Methods* 5 (2008) 763-775.
- 320 [21] W.R. Algar, U.J. Krull, Quantum dots as donors in fluorescence resonance energy
321 transfer for the bioanalysis of nucleic acids, proteins, and other biological molecules,
322 *Analytical and Bioanalytical Chemistry* 391 (2008) 1609-1618.
- 323 [22] G. Beane, K. Boldt, N. Kirkwood, P. Mulvaney, Energy Transfer between Quantum
324 Dots and Conjugated Dye Molecules, *Journal of Physical Chemistry C* 118 (2014)
325 18079-18086.
- 326 [23] S. Bae, H. Kim, Y. Lee, X.F. Xu, J.S. Park, Y. Zheng, J. Balakrishnan, T. Lei, H.R. Kim,
327 Y.I. Song, Y.J. Kim, K.S. Kim, B. Ozyilmaz, J.H. Ahn, B.H. Hong, S. Iijima, Roll-to-roll
328 production of 30-inch graphene films for transparent electrodes, *Nature Nanotechnology*
329 5 (2010) 574-578.
- 330 [24] G. Lalwani, J.L. Sundararaj, K. Schaefer, T. Button, B. Sitharaman, Synthesis,
331 characterization, in vitro phantom imaging, and cytotoxicity of a novel graphene-based
332 multimodal magnetic resonance imaging-X-ray computed tomography contrast agent,
333 *Journal of Materials Chemistry B* 2 (2014) 3519-3530.
- 334 [25] W. Liu, Q.B. Lu, N. Cui, H. Li, L.Y. Wang, K. Liu, Z.D. Yang, B.J. Wang, H.Y. Wang,
335 Y.Y. Zhang, L. Zhuang, C.Y. Hu, C. Yuan, X.J. Fan, Z. Wang, L. Zhang, X.A. Zhang,
336 D.H. Walker, W.C. Cao, Case-Fatality Ratio and Effectiveness of Ribavirin Therapy
337 Among Hospitalized Patients in China Who Had Severe Fever With Thrombocytopenia
338 Syndrome, *Clinical Infectious Diseases* 57 (2013) 1292-1299.

- 339 [26] J.H. Shen, H.N. Zheng, X.H. Zhi, Y.W. Shi, Y. Huang, W. Wang, Y.Q. Chen, J.Q. Kong,
340 P. Zhu, Improvement of Amorpha-4,11-diene Production by a Yeast-Conform Variant of
341 Vitreoscilla Hemoglobin, *Zeitschrift Fur Naturforschung Section C-a Journal of*
342 *Biosciences* 67 (2012) 195-207.
- 343 [27] F.H. Li, J.F. Song, H.F. Yang, S.Y. Gan, Q.X. Zhang, D.X. Han, A. Ivaska, L. Niu, One-
344 step synthesis of graphene/SnO₂ nanocomposites and its application in electrochemical
345 supercapacitors, *Nanotechnology* 20 (2009).
- 346 [28] Z.Z. Wu, W.Y. Li, J. Chen, C. Yu, A graphene quantum dot-based method for the highly
347 sensitive and selective fluorescence turn on detection of biothiols, *Talanta* 119 (2014)
348 538-543.
- 349 [29] Y.L. Jiang, Z.Y. Wang, Z.H. Dai, Preparation of Silicon-Carbon-Based
350 Dots@Dopamine and Its Application in Intracellular Ag⁺ Detection and Cell Imaging,
351 *Acs Appl Mater Inter* 8 (2016) 3644-3650.
- 352 [30] S.H. Li, Y.C. Li, J. Cao, J. Zhu, L.Z. Fan, X.H. Li, Sulfur-Doped Graphene Quantum
353 Dots as a Novel Fluorescent Probe for Highly Selective and Sensitive Detection of Fe³⁺,
354 *Analytical Chemistry* 86 (2014) 10201-10207.
- 355 [31] M.B. Hossain, T. Oshima, S. Hirose, J. Wang, T. Tokumoto, Expression and Purification
356 of Human Membrane Progesterin Receptor alpha (mPR alpha), *Plos One* 10 (2015).
- 357 [32] A.D. Chowdhury, R.A. Doong, Highly Sensitive and Selective Detection of Nanomolar
358 Ferric Ions Using Dopamine Functionalized Graphene Quantum Dots, *Acs Appl Mater*
359 *Inter* 8 (2016) 21002-21010.
- 360 [33] E. Valeur, M. Bradley, Amide bond formation: beyond the myth of coupling reagents,
361 *Chemical Society Reviews* 38 (2009) 606-631.
- 362 [34] T. Oshima, R. Nakayama, S.R. Roy, T. Tokumoto, Purification of the goldfish
363 membrane progesterin receptor alpha (mPRalpha) expressed in yeast *Pichia pastoris*,
364 *Biomed Res* 35 (2014) 47-59.
- 365 [35] T. Tokumoto, M.B. Hossain, J. Wang, Establishment of procedures for studying mPR-
366 interacting agents and physiological roles of mPR, *Steroids* 111 (2016) 79-83.
- 367 [36] T. Tokumoto, M. Tokumoto, P. Thomas, Interactions of diethylstilbestrol (DES) and
368 DES analogs with membrane progesterin receptor-alpha and the correlation with their
369 nongenomic progesterin activities, *Endocrinology* 148 (2007) 3459-3467.
- 370 [37] T. Tokumoto, M. Tokumoto, R. Horiguchi, K. Ishikawa, Y. Nagahama,
371 Diethylstilbestrol induces fish oocyte maturation, *Proceedings of the National Academy*
372 *of Sciences of the United States of America* 101 (2004) 3686-3690.
- 373 [38] T. Tokumoto, M. Tokumoto, Y. Nagahama, Induction and inhibition of oocyte
374 maturation by EDCs in zebrafish, *Reproductive Biology and Endocrinology* 3 (2005).
- 375 [39] T. Tokumoto, T. Yamaguchi, S. Ii, M. Tokumoto, In Vivo Induction of Oocyte
376 Maturation and Ovulation in Zebrafish, *Plos One* 6 (2011).
- 377 [40] M. Nakashima, M. Suzuki, M. Saida, Y. Kamei, M.B. Hossain, T. Tokumoto, Cell-based
378 assay of nongenomic actions of progestins revealed inhibitory G protein coupling to
379 membrane progesterin receptor alpha (mPR alpha), *Steroids* 100 (2015) 21-26.

380

381 **Figure legends**

382 Fig. 1. Preparation of GQD, human mPR α protein and GQD-mPR α . (A) Photograph of
383 prepared GQD solutions. A glass bottle with GQDs solution showed blue color (right panel)
384 comparing with glass bottle with water (left panel) when excited by violet light bulb. (B)

385 Absorbance scanning pattern (magenta) and fluorescent scanning pattern with excitation at
386 360 nm (green) of GQD. The peak of absorbance at 360 nm and fluorescence at 460 nm is
387 indicated by arrows. (C) Western blot analysis of mPR α and GQD-mPR α . The protein band
388 of mPR α is indicated by an arrowhead. The bands of GQD-mPR α are indicated by a bracket.
389 (D) FTIR scanning data of GQD (red line) and GQD-mPR α (blue line) solution.

390 (E) TEM observation of GQD-mPR α . Sizes of observed GQD-mPR α particles were
391 determined and their distribution was summarized.

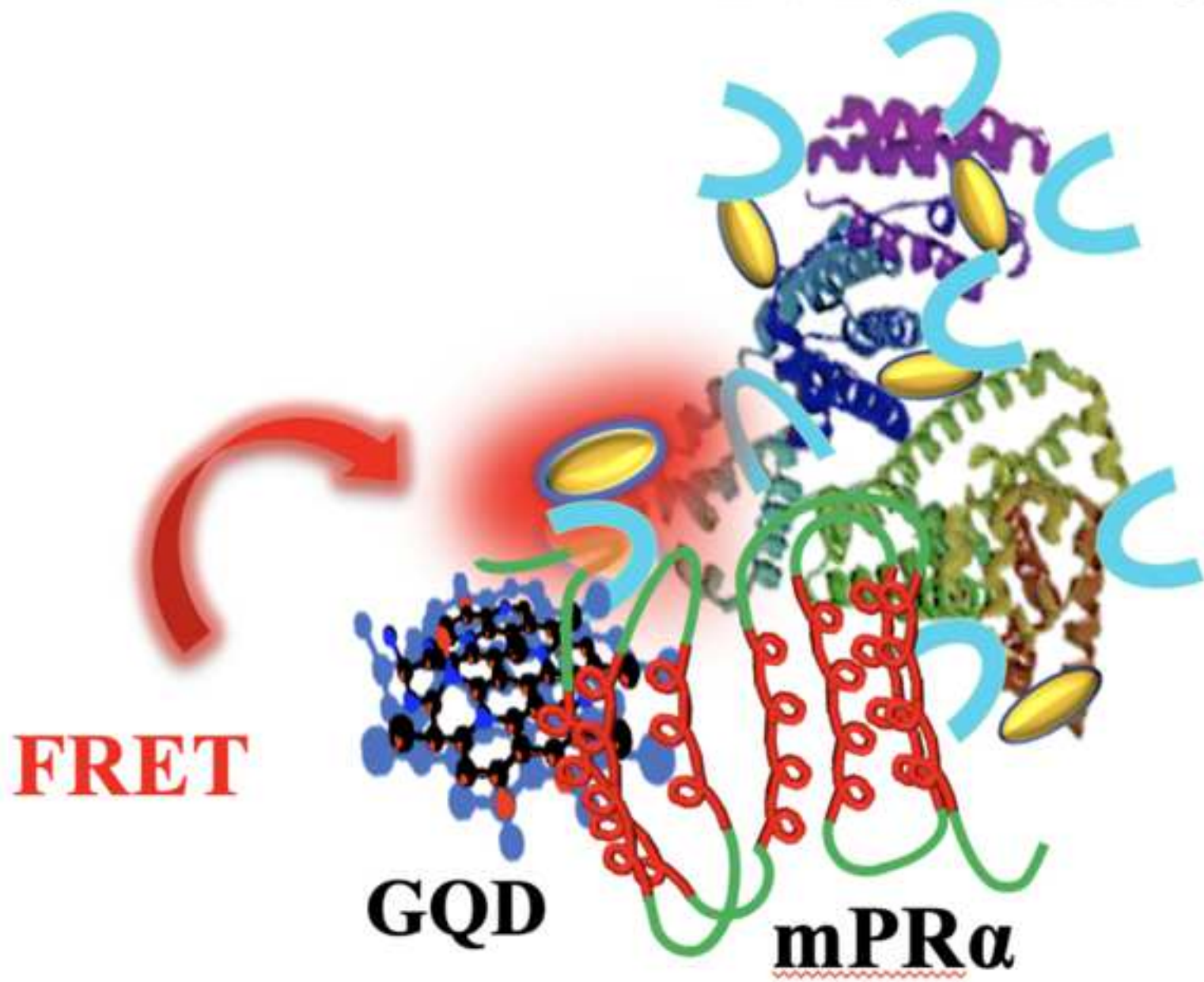
392

393 Fig. 2. Fluorescence characteristics of GQD-mPR α and detection of specific interactions with
394 P4-BSA-FITC. (A) Fluorescent scanning pattern of GQD-mPR α with different excitation
395 wavelengths. The peak of fluorescence at 470 nm is indicated by the arrow. (B) Fluorescent
396 scanning pattern of the reaction mixture with or without free P4. The peak of fluorescence at
397 520 nm is indicated by the arrow. The fluorescence scanning pattern of free GQD-mPR α is
398 also indicated. (C) Measurement of the fluorescence of the reaction mixture under established
399 conditions (Ex 370 nm and Em 520 nm). Fluorescence from GQD-BSA (blue bar) and GQD-
400 mPR α (red bar) mixed with P4-BSA-FITC are compared (P4-BSA-FITC). The effects of the
401 addition of free P4 into the reaction mixture are also indicated (P4-BSA-FITC+P4). (D) The
402 ratios of fluorescence in the absence and presence of free P4 for competitive antagonists are
403 indicated. (E) Competition of the binding of P4-BSA-FITC with GQD-mPR α by steroids and
404 their analogs. The dose-dependent effects of steroids (progesterone (P4), 17 α -
405 hydroxyprogesterone, estradiol-17 β (E2), testosterone (T), cortisol, corticosterone) and their
406 analogs (mifepristone (RU486), methyl-testosterone (Methyl T)) were assayed by the
407 established assay.

408

409 Fig. 3. Schematic diagram of GQD-mPR α and predicted mechanisms of interaction between
410 P4-BSA-FITC. Expected interaction between GQD-mPR α and P4-BSA-FITC (GQD-
411 mPR α +P4-BSA-FITC) is indicated. It is expected that red fluorescence from FITC caused by
412 fluorescence from closed GQDs by the binding of P4-BSA-FITC. The interaction between
413 GQD-mPR α and P4-BSA-FITC is released by free P4, and fluorescence from FITC decreases.
414 Diagrams of each compound (GQD, mPR α , GQD-mPR α , progesterone (P4), FITC are
415 indicated.

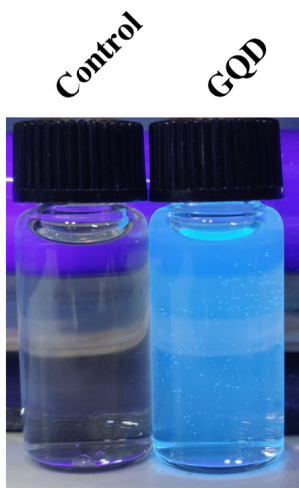
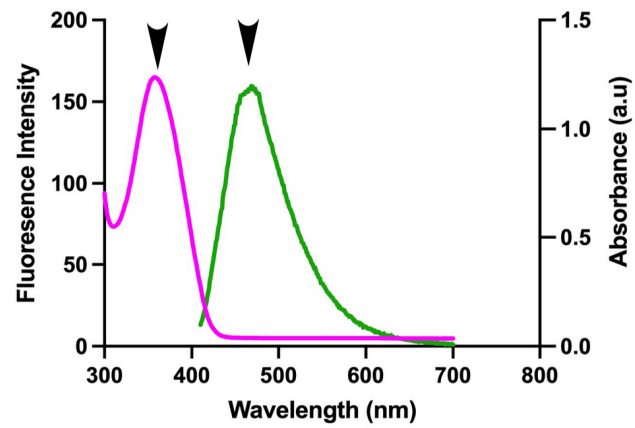
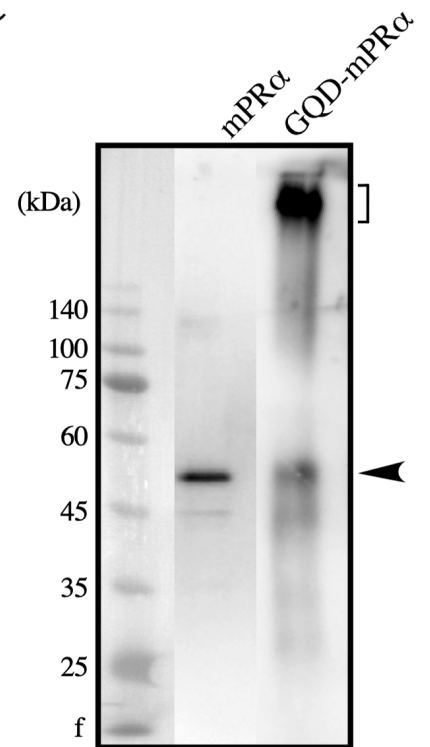
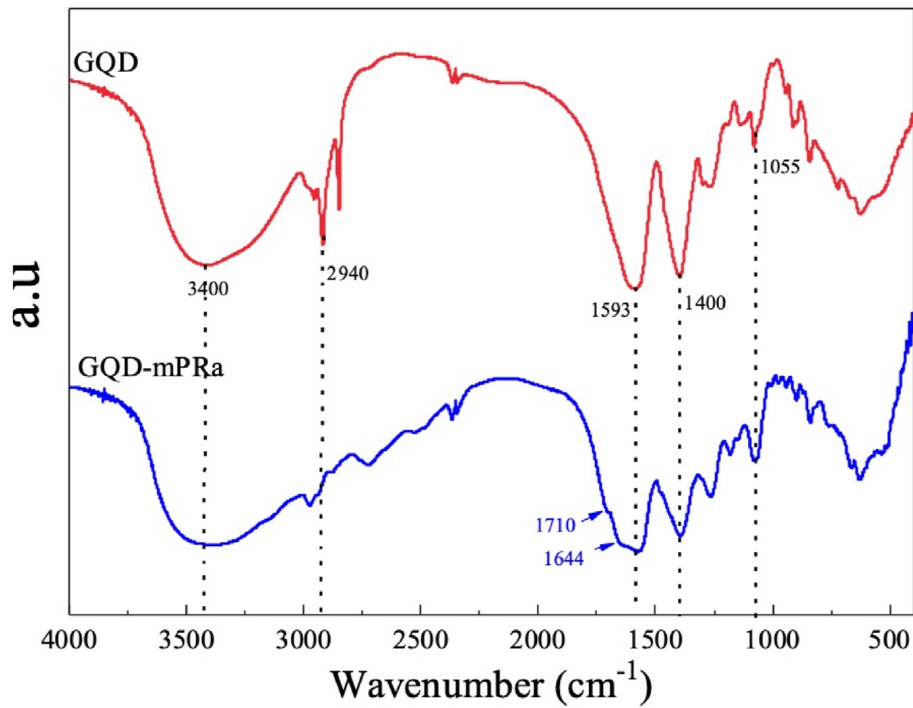
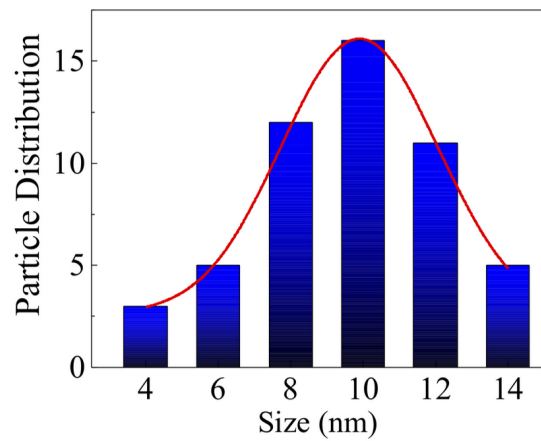
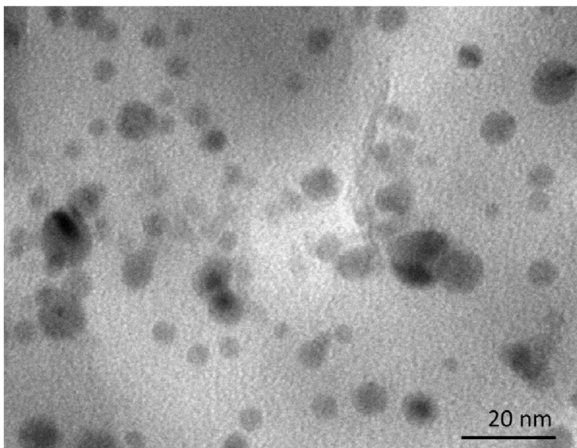
P4-BSA-FITC

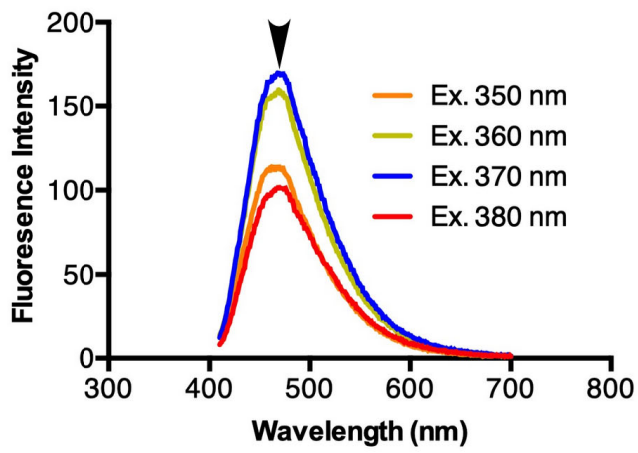
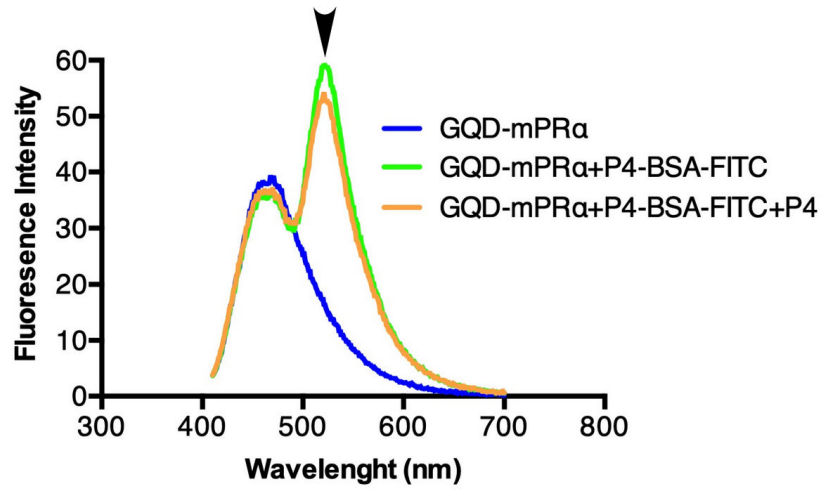
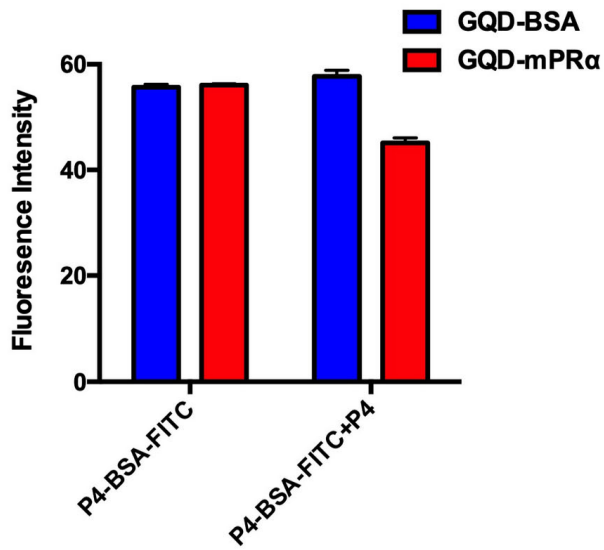
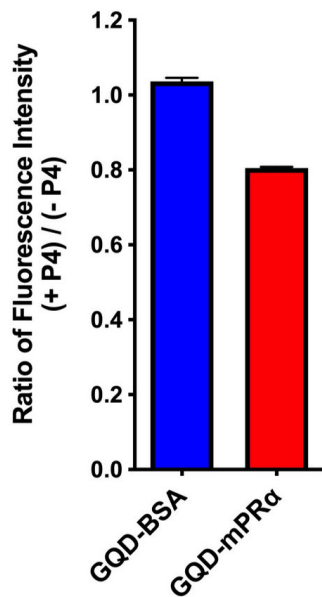


FRET

GQD

mPRα

A**B****C****D****E**

A**B****C****D****E**